Preliminary results on deconfinement phase transition in full QCD

S. Chagdaa[1,*], E. Galsandorj[1], B. Purev[1], O. Kaczmarek[2,3] and H. T. Ding[3]

[1] *Department of Theoretical Physics, Institute of Physics and Technology, Mongolian Academy of Sciences, Peace Ave. 54b, 13330 Ulaanbaatar, Mongolia*

[2] *Fakultät für Physik, Universität Bielefeld, D-33615 Bielefeld, Germany*

[3] *Institute of Particle Physics, Central China Normal University, 152 LuoYu Road, Wuhan 430079*

We explore the profiles of the flux tube connecting a quark and an antiquark in high temperature SU(3) lattice gauge theory in close vicinity to the critical temperature of the phase transition. In this work, we consider the more realistic case of the flux tube with dynamical quarks, extending the previous study to SU(3) gauge group and making use of the Gradient flow method in smoothing procedure for noise reduction. The profiles of the chromoelectric and chromomagnetic field strengths in the flux tube have been measured from Polyakov loop-plaquette correlations using the highly improved staggered quark (HISQ) action on a lattice with temporal extent $N_\tau = 8$. We present preliminary results for distances up to 2.5 fm and temperatures up to $1.09 T_c$.

I. INTRODUCTION

There has been little progress in understanding the flux tube behavior in the presence of dynamical fermions due to the non-locality of the effective lattice action for the gluonic gauge fields. In the effective gauge action the logarithm of the determinant of the fermion matrix appears which becomes more and more non-local for fermions with small mass. In order to avoid this problem early simulations used quenched approximation, but they can not represent the real world.

We present here the profiles of the distribution of chromoelectric and chromomagnetic field components, energy density and width of the flux tube around the deconfinement phase transition in QCD with (2+1) flavors, using HISQ/tree action on a lattice exploiting the Gradient flow method for noise reduction. We work on the line of constant physics, where the strange quark mass is fixed to its physical value m_s at each value of the gauge coupling and the strange to light quark mass ratio is $m_s/m_l = 27$. We present some new preliminary results for interquark distances up to 2.5 fm and temperatures up to $1.09 T_c$.

II. GRADIENT FLOWED CONFIGURATIONS

The configurations have been owed by the flow equation [1, 2]

$$\dot{U}_t(x,\mu) = -g_0^2 \{\partial_{x,\mu} S_W(U_t)\} U_t(x,\mu), \quad U_t(x,\mu)|_{t=0} = U(x,\mu) \tag{1}$$

It introduces extra coordinate t called flow-time and the gauge fields along the flow become smoother with the smearing radius $r_{smear} = \sqrt{8t}$.

If $\partial_{x,\mu}$ is a SU(3)-valued differential operator, calculation of $\partial_{x,\mu} S_W(U_t)$ gives [3]

$$g_0^2 \partial_{x,\mu} S_W(U_t) = \frac{1}{2}(\Omega(x,\rho) - \Omega^+(x,\rho)) - \frac{1}{6} tr(\Omega(x,\rho) - \Omega^+(x,\rho)) \tag{2}$$

where $\Omega(x,\rho) = U(x,\rho) W^+(x,\rho)$ with the staple $W_\rho^+(x)$. Expression in the right hand side of Equation (2) have been constructed from the link variables on the lattice and it makes it convenient to solve Equation (1) numerically for link smearing.

III. FLUX TUBE MEASUREMENT

Polyakov loop-plaquette correlation operators [4,5]

$$f_{\mu,\nu}(R, \boldsymbol{x}) = \frac{\beta}{a^4}\left[\frac{\langle L(0)L^+(R)\rangle_{\mu\nu}^{\dagger}(x)}{\langle L(0)L^+(R)\rangle} - \dagger_{\mu\nu}(\boldsymbol{x}_{ref})\right] \tag{3}$$

measure the chromofield components from the Gradient flowed configurations.
$f_{\mu,\nu}$ is the chromofield strength;

* Electronic address: schagdaa@gmail.com

f_{12}, f_{13} and f_{23} are the space-space components that define chromomagnetic contributions to the chromofield strength;

f_{24}, f_{34} and f_{14} are the space-time components that define chromoelectric contributions to the chromofield strength;

β and a is the gauge coupling constant and lattice spacing.

Polyakov loop:

Table 1. The simulation parameters on the lattice.

$N_s^3 \times N_\tau$	β	T [MeV]	T/T_c	a [fm]	$m_l a$	$m_s a$	N_{conf}	R/a
$32^3 \times 8$	6.390	156.5	0.97	0.156	0.0257	0.694	1150	$4-6$
$32^3 \times 8$	6.423	161.9	1.00	0.150	0.0248	0.670	1150	$4-6$
$32^3 \times 8$	6.445	165.7	1.03	0.147	0.0241	0.652	1150	$4-6$
$32^3 \times 8$	6.474	170.7	1.06	0.142	0.0234	0.632	1150	$4-6$
$32^3 \times 8$	6.500	175.3	1.09	0.139	0.0228	0.614	1150	$4-6$

$$L(\vec{n}) \equiv \frac{1}{N_c}\operatorname{Tr}\prod_{\tau=1}^{N_\tau} U_4(\vec{n},\tau) \qquad (4)$$

The simulation parameters have been summarized in Table 1. The Jackknife method has been used to get the estimates of the statistical errors.

IV. SCALING FUNCTION

To set the lattice spacing we used f_K scaling as determined in Appendix B of [6] with the coefficients $c_0^K = 7.49415$, $c_2^K = 46049$ and $d_2^K = 3671$ updated by 2018. Here one fits af_K data to the Ansatz

$$af_k(\beta) = \frac{c_0^K f(\beta) + c_2^K(10/\beta)f^3(\beta)}{1 + d_2^K(10/\beta)f^2(\beta)} \qquad (5)$$

where

$$f(\beta) = (b_0(10/\beta))^{-b_1/(2b_0^2)}\exp(-\beta/(20b_0))$$

and b_0 and b_1 are the coefficients of the universal two-loop beta functions. Then we can express lattice spacing in fm

$$a(\beta) = af_K(\beta) \cdot \frac{197.3 \text{ MeV} \cdot \text{fm}}{156.1/\sqrt{2} \text{ MeV}} \qquad (6)$$

and temperature in MeV

$$T(\beta, N_\tau) = \frac{156.1/\sqrt{2} \text{ MeV}}{af_K(\beta) \cdot N_\tau}. \qquad (7)$$

Temperatures are in units of the critical temperature

$$\frac{T}{T_c} = \frac{T(\beta, N_\tau)}{T_c(\beta_c, N_\tau)} \equiv \frac{af_K(\beta_c)}{af_K(\beta)}. \qquad (8)$$

The lattice spacing and physical temperatures defined with this scaling function are listed in Table 1.

V. RESULTS

A. Chromofield strength components

Comparison of the strength of the four components $1/2E_{\parallel}^2$, $1/2E_{\perp}^2$, $-1/2B_{\parallel}^2$ and $-1/2B_{\perp}^2$ in the confinement and deconfinement regions is shown in Figure 1. All chromofield components decrease with increasing transverse distance $x_\perp$ and in the confinement region the four components obey the relation

$$E_{\parallel}^2 > E_{\perp}^2 > |B_{\perp}^2| \approx |B_{\parallel}^2|$$

while in the deconfinement region that is shown in the second row of the figure they obey the relation

$$E_{\parallel}^2 > E_{\perp}^2 \approx |B_{\perp}^2| > |B_{\parallel}^2|.$$

The results could suggest that the flux tube with the length of 0.9 fm does exist in the region with temperature $T = 1.03T_c$ as shown in Figure 1. We see from the figure that there is obviously no flux tube at $T = 1.09T_c$ and $R = 2.2$ fm.

Effect of the Gradient flow: Figure 2 shows the strength of the chromofield components on the middle point ($x_{\parallel} = R/2, x_\perp = 0$) between $q\bar{q}$ pair as a function of the flow-time value. Transverse profiles of the parallel chromoelectric and chromomagnetic components at the midplane ($x_{\parallel} = R/2, x_\perp$) have been plotted at the fixed distance $R = 0.6$ fm for different temperatures in Figure 3. The both parallel chromofield components decrease with increasing transverse distance $x_\perp$ and vanishes at about $x_\perp = 0.7$ fm for all temperatures. Unlike the

parallel chromoelectric component the strength of the parallel chromomagnetic component has a tendency to increase as a function of temperature. The strength on the middle point ($x_\parallel = R/2, x_\perp = 0$) as functions of the interquark distance and temperature is plotted in Figure 4. The strength of the both parallel chromofield components in the middle region between $q\bar{q}$ pair clearly decreases with increasing interquark distance at all temperatures. Distance at which they vanish seems to meet the value around $R = 1.2$ fm, which is expected to be the distance of flux tube disappearance at zero temperature [7]. This might hold also at high temperature.
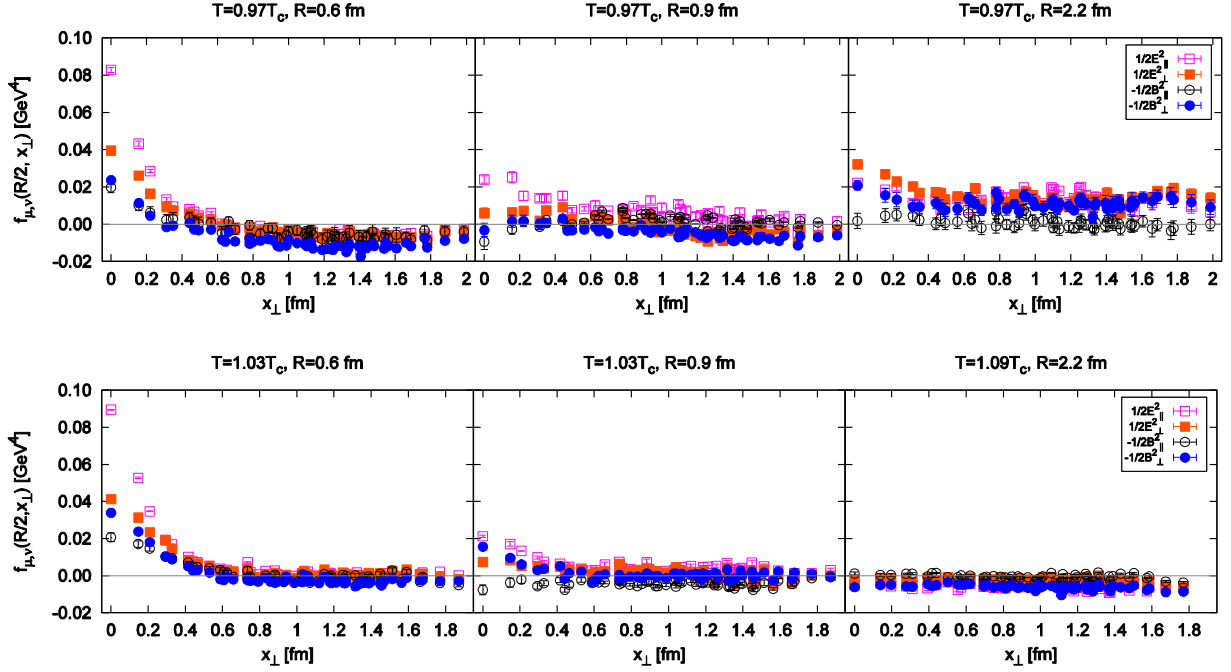

Figure 1. Comparison of the strength of the chromofield components in the confinement and deconfinement regions at different distances from a lattice of size $32^3 \times 8$.
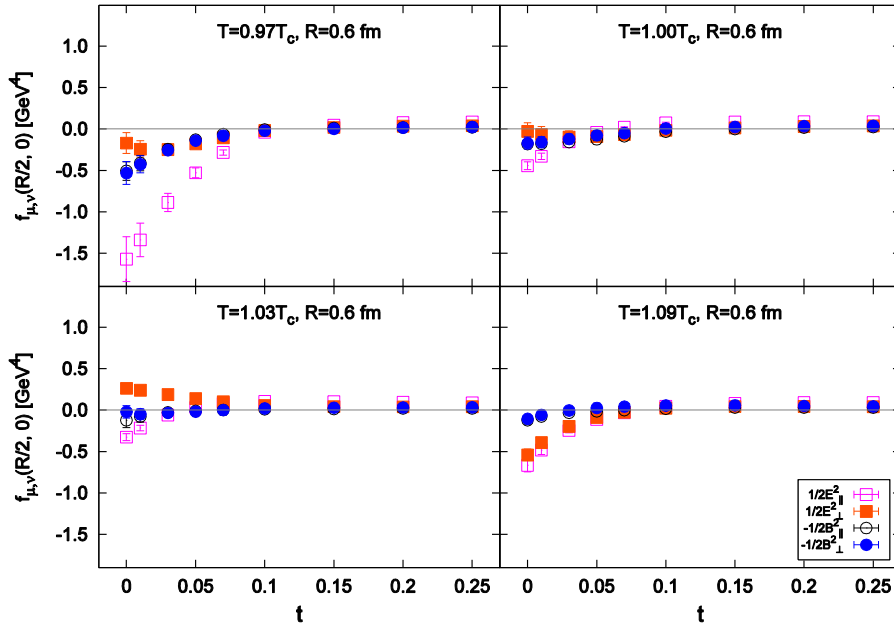

Figure 2. The behavior of the operator (3) vs smoothing by Gradient flow method on a $32^3 \times 8$ lattice. The dependence is drawn for different temperatures at the fixed distance R = 0.6 fm.

In the confinement phase the strength of the both chromofield components increase with temperature until it reaches T_c. In the deconfinement phase, above T_c, they decrease with temperature and vanish at a different temperature for a given distance value, namely at a lower temperature for a larger distance. Chromoelectric flux tubes with the length of less

than 1.2 fm do seem to survive the phase transition showing the non-vanishing values in the deconfinement phase, while in the magnetic sector only flux tubes with the length of 0.56 fm is remained.
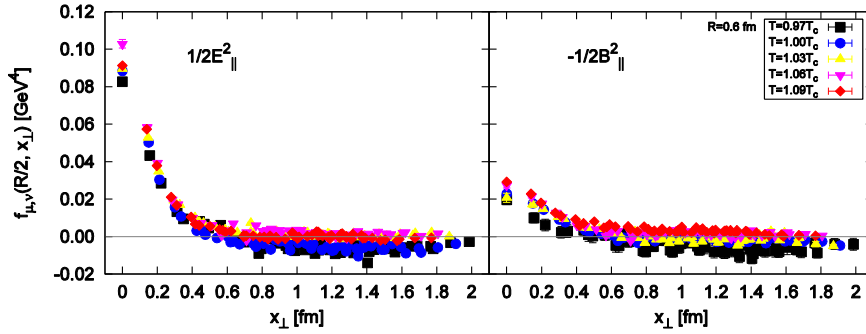

Figure 3. Transverse profiles of the parallel chromoelectric and chromomagnetic components at the midplane ($x_\parallel = R/2, x_\perp$) at the fixed distance $R = 0.6$ fm for different temperatures from the lattice of size $32^3 \times 8$.
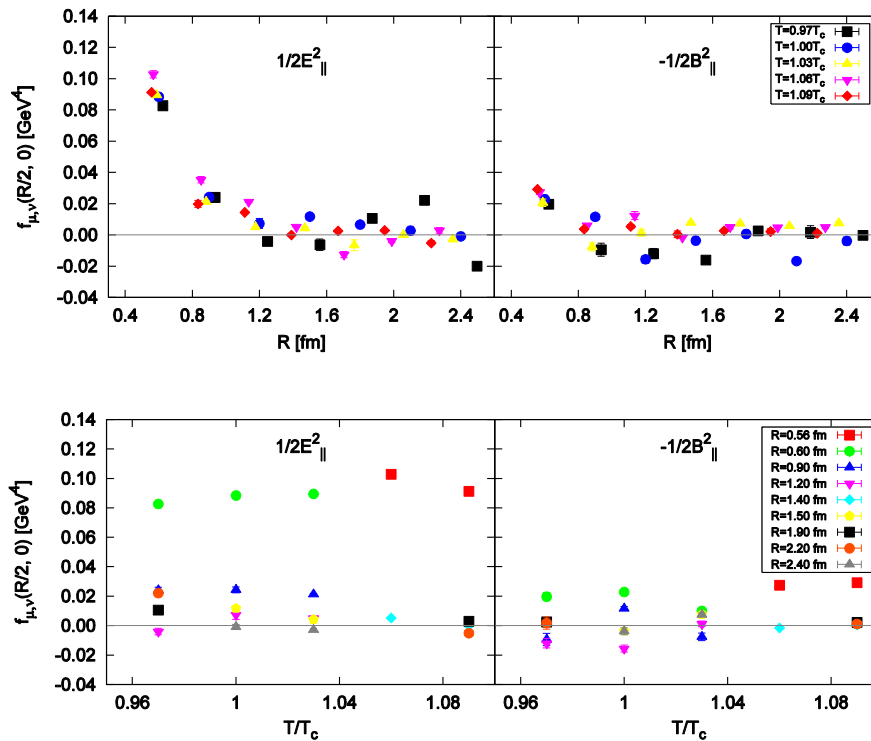

Figure 4. The strength at $x_\perp = 0$ point on Figure 3 as functions of the interquark distance and temperature.

B. Energy density in the flux tube

Total magnetic and electric chromofield strengths which are, respectively,

$$\mathcal{M} = -(f_{12} + f_{13} + f_{23})$$
$$\mathcal{E} = f_{24} + f_{34} + f_{14} \qquad (8)$$

define the total energy density as

$$\varepsilon = \mathcal{E} + \mathcal{M} \qquad (9)$$

We present in Figure 5 longitudinal and transverse distribution of the energy density ε calculated with the Equation (9) as functions of interquark distance and temperature. The energy density in the middle region between the quark and antiquark clearly decreases with increasing interquark distance. We also see a decreasing energy density with temperature. To show them in more detail Figure 6 presents value of the energy density at the midpoint

$(x_\parallel = R/2, x_\perp = 0)$ as functions of the interquark distance and temperature. In the confinement phase the energy density of the flux tube decreases when temperature approaches T_c from below. In the deconfinement phase the energy density further decreases with temperature at all distances. We see from the plot that the flux tubes with length of less than 2.2 fm do still survive for temperatures up to $1.09T_c$. Thus we find string breaking distance to be around 2.2 fm in the region with temperature $1.09T_c$ in full QCD.
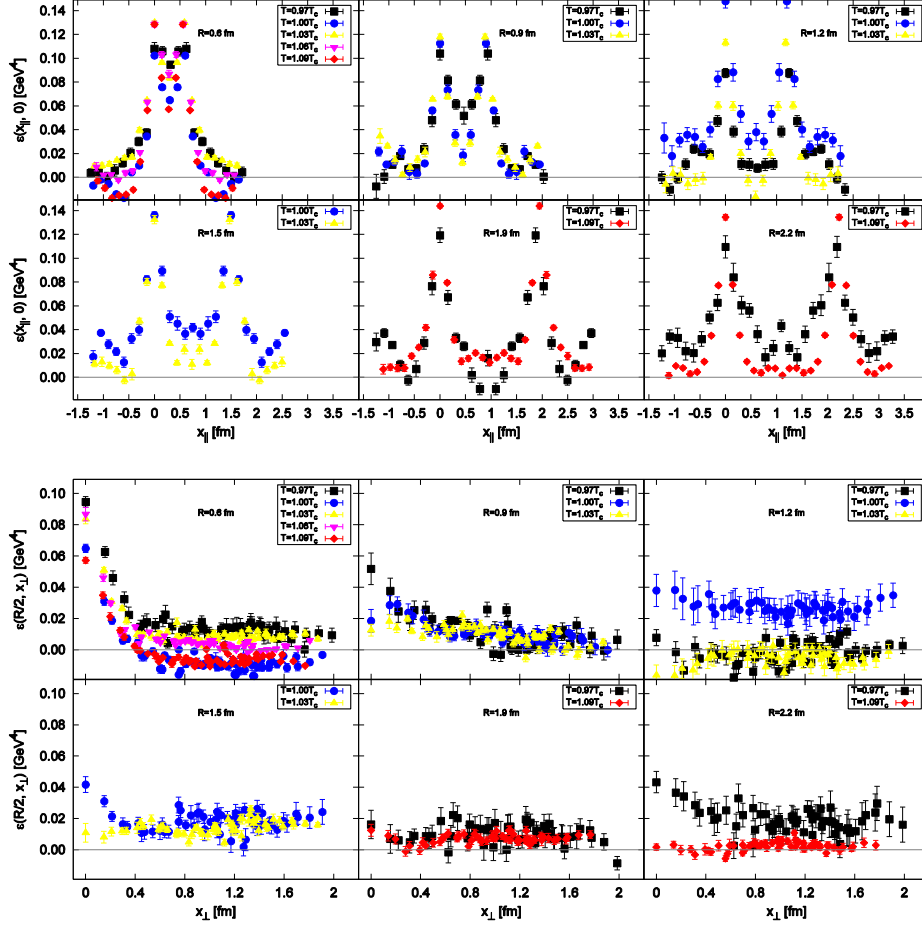

Figure 5. Longitudinal and transverse distribution of the energy density in the flux tube as functions of interquark distance and temperature from the lattice of size $32^3 \times 8$.
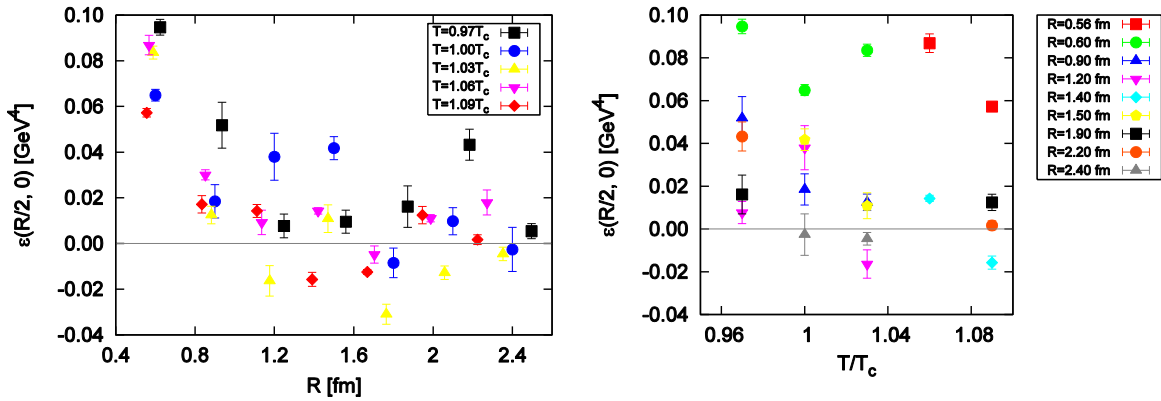

Figure 6. The energy density value at the point $(x_\parallel = R/2, x_\perp = 0)$ *on Figure 5 as functions of the interquark distance and temperature.*

C. Width of the flux tube

We define physical width of the flux tube as width of its energy density and estimate it quantitatively by fitting the middle transverse distribution of the energy density to an exponential function [8].

$$f(x_\perp) = a_1 e^{-a_2 x_\perp} + K \qquad (10)$$

from that the width D_ε has been computed via

$$D_\varepsilon^2/a^2 = \frac{\int d^2 x_\perp x_\perp^2 (f(x_\perp) - K)}{\int d^2 x_\perp (f(x_\perp) - K)} \qquad (11)$$

in terms of the fitting parameters a_1 and a_2.

Table 2. The fit results for quadratic width of the flux tube.

β	R	χ^2/ndf	a_1	a_2	K	D_ε^2/a^2
	4	0.86	0.00550(19)	0.708(48)	0.000668(47)	11.96(1.61)
6.390	6	2.14	0.00265(53)	0.310(89)	0.000283(145)	62.39(35.96)
	14	0.63	0.00173(32)	0.601(203)	0.001113(75)	16.63(11.24)
	4	6.32	0.00393(32)	0.639(73)	−0.000478(52)	14.71(3.36)
6.423	6	0.75	0.00136(16)	0.213(72)	0.000174(141)	131.75(89.15)
	8	0.22	0.00076(23)	0.483(206)	0.001397(46)	25.68(21.86)
	10	1.19	0.00144(30)	1.286(401)	0.000956(43)	3.63(2.26)
6.445	4	2.60	0.00405(21)	0.869(53)	0.000399(22)	7.95(97)
	4	7.01	0.00343(40)	0.755(71)	0.000094(21)	10.52(1.99)
6.474	6	3.06	0.00100(135)	0.391(103)	0.000265(44)	39.27(20.65)
	14	3.24	0.00062(12)	1.038(249)	0.000092(19)	5.57(2.67)
	4	9.83	0.00268(22)	0.769(77)	0.000257(17)	10.15(2.04)
6.500	6	4.57	0.00061(20)	0.343(134)	0.000008(35)	50.91(39.65)
	8	3.14	0.00068(19)	1.053(496)	−0.000077(22)	5.42(5.10)

The resulting values of the fit parameters and width in lattice units are listed in Table 2. The width of the energy density D_ε as functions of the distance R and temperature T is displayed in Figure 7 in physical units. Width of the flux tube increases with interquark distance until the distance reaches around 0.9 fm, after which it strongly decreases with further increasing distance. The presence of dynamical quarks seems to widen the flux in a small distance up to around $R = 0.9$ fm but to suppress it with further separation which could be

an indication of hadronization.

Temperature dependence of the width at a fixed distance is shown in the second plot of Figure 7 for various distances. We see that the width of the flux tube increases as a function of temperature up to T_c. In the deconfinement phase it tends to decrease with temperature: but at our highest temperature a flux tube with length of 1.1 fm is giving some non-zero width, while a longest flux tube with length of 2 fm is giving non-zero width at $1.06 T_c$.
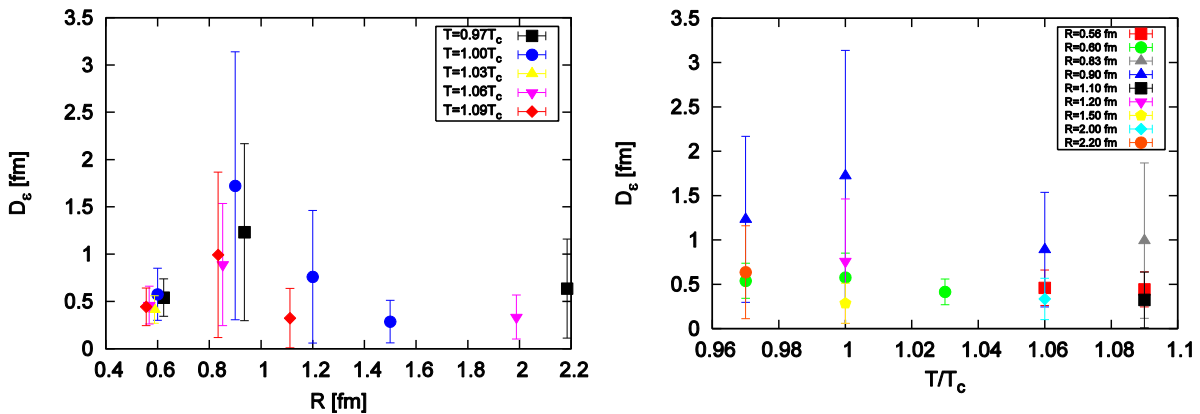

Figure 7. The width of the flux tube as functions of the interquark distance and temperature from the lattice of size $32^3 \times 8$.

VI. CONCLUSION

We have studied behavior of the flux tube produced by a static quark-antiquark pair in full QCD with (2+1) flavors across the deconfinement phase transition. We have performed simulations with HISQ/tree action on a lattice exploiting the Gradient flow method for noise reduction. We work on the line of constant physics, where the strange quark mass is fixed to its physical value m_s at each value of the gauge coupling and the strange to light quark mass ratio is $m_s/m_l = 27$.

We find that the width of the flux tube does not always increase as a function of distance in both confined and deconfined phases when the dynamical fermions are presented. In both phases it increases with distance up to the distance around $R = 0.9$ fm after which it is strongly suppressed due to the dynamical fermions.

The decreases of the both energy density and width of the flux tube with temperature above the T_c suggest that flux tube structure melts eventually beyond certain distance and temperature value in the deconfined phase. Our study in the presence of dynamical fermions shows that flux tube structures with length of 2 fm persists up to temperature $1.06T_c$ and flux tubes with length of 1.1 <u>fm</u> persists up to temperature $1.09T_c$. These are in qualitative agreement with the conclusion in [9] that the flux tube structure survives to the deconfinement transition and conclusion in [10] that in presence of dynamical fermions for a sufficiently large distance between sources the flux tube structure disappears.

ACKNOWLEDGMENTS

REFERENCES

[1] M. Lüscher, Properties and uses of the Wilson flow in lattice QCD, JHEP 08 (2010) 071, [arXiv:hep-lat/1006.4518].

[2] M. Lüscher, Trivializing maps, the Wilson flow and the HMC algorithm, Comm. Math. Phys. 293 (2010) 899-919, [arXiv:hep-lat/0907.5491].

[3] L. Mazur, Applications of the Gradient flow method in lattice QCD, Master's thesis, Bielefeld University (2017).

[4] M. Fukugita and T. Niuya, The distribution of chromoelectric flux in SU(2) Lattice Gauge Theory, Phys. Lett. 132B (1983) 374-378.

[5] S. Chagdaa, E. Galsandorj, E. Laermann and B. Purev, Width and string tension of the flux tube in SU(2) lattice gauge theory at high temperature, J. Phys. G 45 (2017) 025002.

[6] A. Bazavov et al., Chiral and deconfinement aspects of the QCD transition, Phys. Rev. D 85 (2012) 054503.

[7] K. Schilling, Review on string breaking - the query in quest of the evidence, Nucl. Phys. B (Proc. Suppl.) 83 (2000) 140-145 and references therein.

[8] R. Sommer, Chromoflux distribution in lattice QCD, Nucl. Phys. B291 (1987) 673-691.

[9] P. Cea, L. Cosmai, F. Cuteri and A. Papa, Flux tubes at finite temperature, JHEP 06 (2016) 033, [arXiv:hep-lat/1511.01783].

[10] L. Cosmai, P. Cea, F. Cuteri and A. Papa, Flux tubes in QCD with (2+1) HISQ fermions, PoS (LATTICE2016) (2016) 344, [arXiv:hep-lat/1701.03371].